Two new phosphate langbeinites, Rb$_2$YbTi(PO$_4$)$_3$ and Rb$_2$Yb$_{0.32}$Ti$_{1.68}$(PO$_4$)$_3$, investigated at 293 and 150 K

Joacim C. M. Gustafsson,[a]* Stefan T. Norberg,[b] Göran Svensson[a] and Jörgen Albertsson[a]

[a]Department of Materials and Surface Chemistry, Solid State Chemistry, Chalmers University of Technology, SE-412 96 Göteborg, Sweden, and [b]Ceramics Research Laboratory, Tajimi, 507-0071 Gifu, Japan

Correspondence e-mail: jogu@chem.chalmers.se

The rubidium ytterbium titanium phosphates Rb$_2$YbTi(PO$_4$)$_3$, (I), and Rb$_2$Yb$_{0.32}$Ti$_{1.68}$(PO$_4$)$_3$, (II), have been structurally characterized from X-ray data collected at both 293 and 150 K. Compound (II) is blue owing to the presence of mixed-valence titanium (41% Ti^{3+} + 59% Ti^{4+}). Both (I) and (II) belong to the langbeinite structure type, with mixed Yb/Ti populations in the two crystallographically independent octahedral sites (of symmetry 3). Ytterbium favours one of these sites, where about two-thirds of the Yb atoms are found. The O-atom displacement parameters are large in both compounds at both temperatures.

Comment

KTP (KTiOPO$_4$) and its analogues RTP (RbTiOPO$_4$) and CTA (CsTiOAsO$_4$) are well known ferroelectric materials with excellent non-linear optical properties (Satyanarayan *et al.*, 1999). The optical properties of these compounds can be changed by modifying the composition, for example, by replacing some of the titanium in RTP by ytterbium. In an attempt to prepare ytterbium-doped RTP by adding Yb$_2$O$_3$ to the flux, crystals of RTP were grown. Simultaneously, well shaped colourless tetrahedral crystals were found, a small number of them showing a blue colour. Upon analysis, these crystals were found to belong to the langbeinite structure type. All examined crystals from the same growth experiment had one of two compositions, *viz.* Rb$_2$YbTi(PO$_4$)$_3$ (colourless), (I), or Rb$_2$Yb$_{0.32}$Ti$_{1.68}$(PO$_4$)$_3$ (blue), (II). Differential scanning calorimetry (DSC) indicated a phase transition at 183 K for (I). We present here a detailed crystallographic investigation of the two new phosphate langbeinites at two different temperatures.

The title compounds belong to the large group of synthetic $A_xM_2(XO_4)_3$ compounds named after the mineral langbeinite, *viz.* K$_2$Mg$_2$(SO$_4$)$_3$ (Zemann & Zemann, 1957). Langbeinite compounds have attracted a significant amount of interest because of their ferroelectric and ferroelastic behaviour, for example, (NH$_4$)$_2$Cd$_2$(SO$_4$)$_3$ (Jona & Pepinsky, 1956), Tl$_2$Cd$_2$(SO$_4$)$_3$ (Brezina & Glogarova, 1972) and K$_2$Cd$_2$(SO$_4$)$_3$ (Abrahams & Bernstein, 1977). All known langbeinites crystallize in a common high-temperature cubic phase, in space group $P2_13$. Below room temperature, most of them undergo one or several phase transitions, with two possible transitions paths. The first path includes several steps from $P2_13$ to the final orthorhombic space group $P2_12_12_1$, as exemplified by the phase transitions of Tl$_2$Cd$_2$(SO$_4$)$_3$ (Brezina & Glogarova, 1972; Guelylah *et al.*, 2000): $P2_13$ (RT) $\rightarrow$ $P2_1$ (128 K) $\rightarrow$ P1 (119 K) $\rightarrow$ $P2_12_12_1$ (98 K).

In the second path, the transformation proceeds directly from the high-temperature $P2_13$ phase to the orthorhombic low-temperature $P2_12_12_1$ phase. Several different mechanisms for these transitions have been suggested (*e.g.* Percival *et al.*, 1989; Moriyoshi *et al.*, 1996).

Phosphate langbeinites containing titanium form a small group of compounds, including KTi$_2$(PO$_4$)$_3$, K$_2$Ti$_2$(PO$_4$)$_3$, K$_{1+x}$Ti$_{2-y}$Al$_y$(PO$_4$)$_3$, K$_2$MTi(PO$_4$)$_3$ (M = Er, Yb or Y) and Rb$_2$ErTi(PO$_4$)$_3$ (Masse *et al.*, 1972; Leclaire *et al.*, 1989; Slobodyanik *et al.*, 1991; Norberg, 2002; Carvajal *et al.*, 2003). Some of these compounds contain mixed-valence octahedral cations, such as Ti^{3+}/Ti^{4+} in K$_2$Ti$_2$(PO$_4$)$_3$. This is also the case for the present compound (II). The small number of phosphate langbeinites is a result of the fact that most A_xM_2(PO$_4$)$_3$ compounds tend to crystallize in the closely related nasicon structure, Na$_3$Zr$_2$(PO$_4$)(SiO$_4$)$_2$ (Sljukic *et al.*, 1967; von Alpen *et al.*, 1979). There are also examples of the same compound crystallizing in both the langbeinite and the nasicon structure (Masse *et al.*, 1972). One important difference between the two structures is that, in langbeinites, the alkali cations are
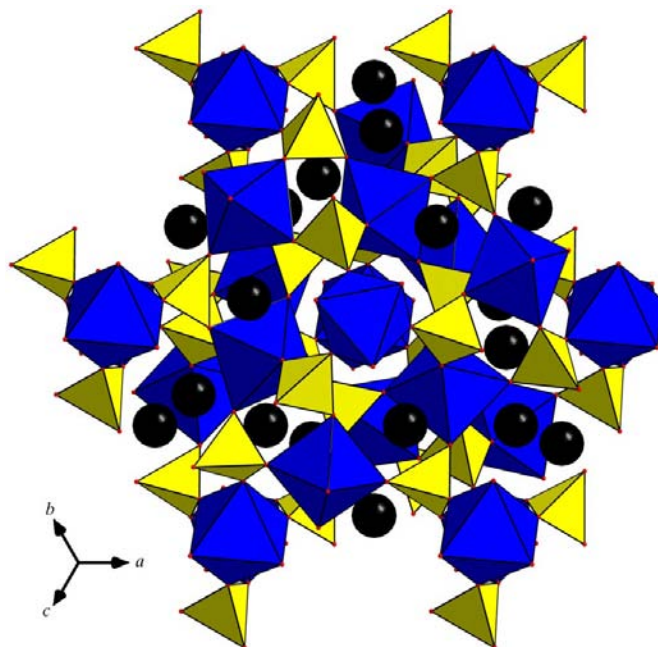

Figure 1
A polyhedral view of the Rb$_2$YbTi(PO$_4$)$_3$ structure along (111).

inorganic compounds

located in cages, while in nasicon, they are found in tunnels. The langbeinite framework is built of MO_6 octahedra sharing corners with PO_4 tetrahedra (Fig. 1). An alternative description of the framework is based on $[M_2X_3O_{18}]$ units composed of two MO_6 octahedra linked together by three XO_4 tetrahedra. Another description based on $M_5X_6O_{39}$ units, which has recently been presented by Norberg (2002), gives an improved visualization of the cages and tunnels formed in langbeinite and nasicon, respectively. An alternative description of the langbeinite structure, in terms of packed ⟨111⟩ rods, has been given by O'Keeffe & Andersson (1977).

Within the langbeinite framework, large cages are formed, in which the alkali cations are located. Each cage contains two Rb^+ ions separated by 3.917 (1) and 3.932 (2) Å at room temperature in (I) and (II), respectively. These distances are longer than the sum of the ionic radii for nine-coordinate Rb^+ ions (3.38 Å; Shannon, 1976). The cages have a volume of approximately $5 \times 5 \times 11$ Å and are isolated from one another, making langbeinites poor ionic conductors. The $Rb1^+$ and $Rb2^+$ cations are best described as 12- and nine-coordinate, respectively. Atom Rb1 can also be described as being surrounded by four MO_6 octahedra in a tetrahedral arrangement, while atom Rb2 is surrounded by six MO_6 octahedra in an octahedral geometry. These large polyhedra are regular and share one triangular face to form a cage of seven MO_6 octahedra about two Rb^+ ions (Fig. 2). The Rb—M distances in the cage are in the range 3.85–3.97 Å. The arrangement of the seven MO_6 octahedra around the Rb atoms results in an opening in the cage located opposite the tetrahedron. This opening is closed by an eighth octahedron, at an M—Rb distance of about 5.15 Å for both compounds at both temperatures. Thus, the two Rb atoms are located at one end of the cage with room to accommodate another small cation in the empty part of the cage (Fig. 2). To the best of our knowledge, no langbeinite structure has yet been found in which all three positions are occupied. Bond-valence sums

(Brown, 1981; Brown & Altermatt, 1985) for (I) and (II) have been calculated (Table 2). The difference between the two Rb sites reflects the difference in coordination, and the lower bond-valence sum for Rb2 indicates underbonding.

Selected bond distances for the two compounds are given in Table 1. The two crystallographically independent MO_6 ($M =$ Ti/Yb) octahedra are regular, with the metal atom slightly off-centre by 0.0380 (8) (M1) and 0.0707 (9) Å (M2) in (I), and 0.050 (2) (M1) and 0.0564 (8) Å (M2) in (II). The centre of the octahedra was calculated as the geometric mean for the six O-atom positions at the vertices.

The distribution between the Ti and Yb atoms is not equal in the two octahedral sites, as two-thirds of the Yb atoms are found in the $M1O_6$ octahedra and one-third are found in the $M2O_6$ octahedra. The $M1O_6$ octahedra define the shared triangular face between the Rb2 $(MO_6)_6$ octahedra and the Rb1 $(MO_6)_4$ tetrahedra (Fig. 2). The $M1O_6$ octahedra are thus more influenced by the Rb^+ cations than the $M2O_6$ octahedra, and this might have an impact on the distribution of Yb.

The geometry of the phosphate groups in (I) and (II) is as expected. The displacement parameters for the O atoms are large and the ellipsoids are mostly oriented with the major axis perpendicular to the P—O bond (Fig. 3). This result is an indication of O-atom disorder or rotation of the phosphate group, which has been interpreted as the initial stages of a phase transition in langbeinites (Lissalde *et al.*, 1979). The displacement parameters of the O atoms are not affected by the change in temperature, while those of the metal atoms decrease by approximately 25%. The temperature decrease from 298 to 150 K does not affect the cell parameters and a
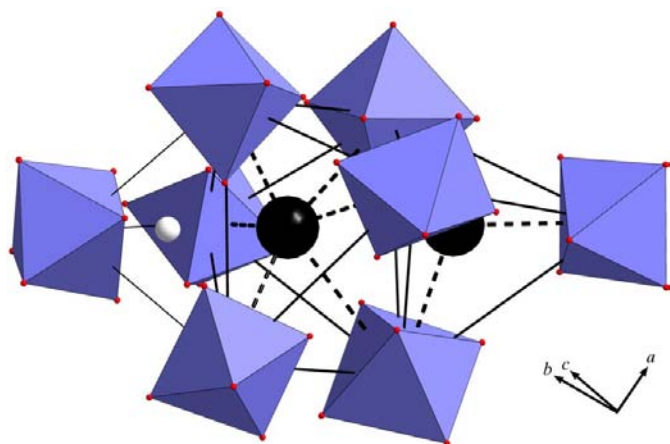

Figure 2
A polyhedral view of $Rb_2YbTi(PO_4)_3$, with phosphate groups omitted for clarity. The cage formed by the MO_6 octahedra around the Rb^+ cations (black spheres) is outlined. A third possible cation site (white sphere) is indicated.
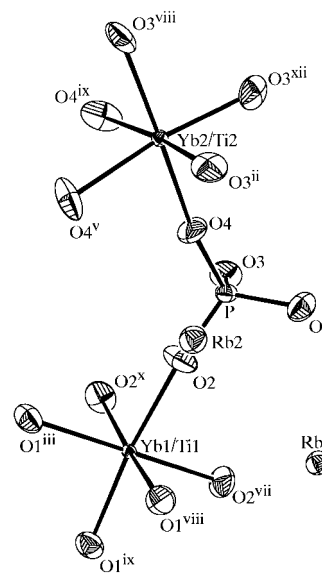

Figure 3
Part of the $Rb_2YbTi(PO_4)_3$ structure, viewed in the [001] direction. Displacement ellipsoids are shown at the 50% probability level. [Symmetry codes: (i) $2 - z$, $x - \frac{1}{2}$, $\frac{3}{2} - y$; (ii) $\frac{3}{2} - x$, $1 - y$, $\frac{1}{2} + x$; (iii) $\frac{3}{2} - z$, $1 - x$, $\frac{1}{2} + y$; (iv) $\frac{1}{2} + z$, $\frac{3}{2} - x$, $1 - y$; (v) $2 - x$, $y - \frac{1}{2}$, $\frac{3}{2} - z$; (vi) $2 - y$, $z - \frac{1}{2}$, $\frac{3}{2} - x$; (vii) $\frac{3}{2} - y$, $1 - z$, $x - \frac{1}{2}$; (viii) y, z, x; (ix) $1 - z$, $x - \frac{1}{2}$, $\frac{3}{2} - y$; (x) $1 - y$, $z - \frac{1}{2}$, $\frac{3}{2} - x$.]

slight increase (0.3%) of the cell volume is even observed for (II).

As mentioned above, DSC data indicated a phase transition at 183 K. Data were therefore collected for both compounds at 150 K in order to investigate the formation of a possible low-temperature phase. However, the structure refinements did not reveal a phase transition. In an attempt to obtain an indication of how close these structures are to a phase transition, the instability index GII was calculated [GII is the r.m.s. deviation between the valence sums and oxidation states averaged over all atoms in the structure (Salinas-Sanchez *et al.*, 1992)]. A GII value above 0.05 is an indication of a strained structure (Rao *et al.*, 1998), while structures with values above 0.20 are considered unstable. For both (I) and (II), the calculated GII indices are about 0.10 at 150 K.

Experimental

The crystals of (I) and (II) originated from the same experiment intended to produce modified rubidium titanyl phosphate (RTP; Thomas *et al.*, 1992). They were obtained in a high-temperature solution growth experiment, using a 1:3:2:0.25 molar mixture of TiO_2, $RbCO_3$, NH_4HPO_4 and Yb_2O_3, with a total of 10 g in the batch. The chemicals were mixed carefully in a 35 ml platinum crucible and heated slowly to 1273 K for about 3 d. The melt was then kept at this temperature for 2 d and thereafter cooled slowly to 1023 K at 1.5 K h^{-1}. The crystals were recovered by dissolving the flux in water. The langbeinite crystals were easily separated from RTP on the basis of the difference in morphology. Fewer than 1% of the langbeinite crystals had a blue colour, indicating that Ti^{3+} should be present in these crystals, in agreement with the colour of $K_2Ti_2(PO_4)_3$ (Lunezheva *et al.*, 1989). The reduction of Ti^{4+} to Ti^{3+} during growth means that some oxidation must have occurred, possibly of the platinum crucible; the degree of oxidation appeared to be affected by the flux. Because only a very small amount of (II) was available, it was not possible to verify the amount of Ti^{3+} present. This amount was calculated from the stoichiometric formula obtained during the crystallographic determination. Energy dispersive X-ray analysis (electro-scan S4-8DV equipped with a Link eX1 EDX system) was used in order to verify the atomic content of the crystals used for the structural work. The measurements indicated a Yb/Ti ratio close to 1:1 and a K/P ratio of 2:3 for (I), and a Yb/Ti ratio of about 1:5 for (II).

Compound (I) at 293 K

Crystal data

$Rb_2YbTi(PO_4)_3$	Mo $K\alpha$ radiation
$M_r = 676.79$	Cell parameters from 7163
Cubic, $P2_13$	reflections
$a = 10.2083$ (2) Å	$\theta = 2.8$–33.0°
$V = 1063.80$ (4) Å^3	$\mu = 19.09$ mm^{-1}
$Z = 4$	$T = 293$ (2) K
$D_x = 4.226$ Mg m^{-3}	Plate, colourless
	$0.07 \times 0.06 \times 0.05$ mm

Data collection

Siemens SMART CCD	1338 independent reflections
diffractometer	1326 reflections with $F^2 > 2\sigma(F^2)$
ω scans	$R_{int} = 0.053$
Absorption correction: multi-scan	$\theta_{max} = 33.1°$
(*SADABS*; Sheldrick, 2001)	$h = -15 \rightarrow 15$
$T_{min} = 0.257$, $T_{max} = 0.385$	$k = -15 \rightarrow 15$
19 443 measured reflections	$l = -15 \rightarrow 15$

Refinement

Refinement on F^2	$(\Delta/\sigma)_{max} = 0.001$
$R[F^2 > 2\sigma(F^2)] = 0.024$	$\Delta\rho_{max} = 0.63$ e Å^{-3}
$wR(F^2) = 0.056$	$\Delta\rho_{min} = -1.35$ e Å^{-3}
$S = 1.24$	Absolute structure: Flack (1983),
1338 reflections	570 Friedel pairs
60 parameters	Flack parameter = 0.021 (16)
$w = 1/[\sigma^2(F_o^2) + (0.01P)^2$	
$+ 7.1387P]$	
where $P = (F_o^2 + 2F_c^2)/3$	

Compound (I) 150 K

Crystal data

$Rb_2YbTi(PO_4)_3$	Mo $K\alpha$ radiation
$M_r = 676.79$	Cell parameters from 7527
Cubic, $P2_13$	reflections
$a = 10.2111$ (2) Å	$\theta = 2.8$–32.9°
$V = 1064.68$ (4) Å^3	$\mu = 19.08$ mm^{-1}
$Z = 4$	$T = 150$ (2) K
$D_x = 4.222$ Mg m^{-3}	Plate, colourless
	$0.08 \times 0.07 \times 0.05$ mm

Data collection

Siemens SMART CCD	1342 independent reflections
diffractometer	1333 reflections with $F^2 > 2\sigma(F^2)$
ω scans	$R_{int} = 0.044$
Absorption correction: multi-scan	$\theta_{max} = 33.1°$
(*SADABS*; Sheldrick, 2001)	$h = -15 \rightarrow 15$
$T_{min} = 0.25$, $T_{max} = 0.385$	$k = -15 \rightarrow 15$
19 497 measured reflections	$l = -15 \rightarrow 15$

Refinement

Refinement on F^2	$(\Delta/\sigma)_{max} = 0.001$
$R[F^2 > 2\sigma(F^2)] = 0.023$	$\Delta\rho_{max} = 0.71$ e Å^{-3}
$wR(F^2) = 0.054$	$\Delta\rho_{min} = -1.22$ e Å^{-3}
$S = 1.28$	Absolute structure: Flack (1983),
1342 reflections	574 Friedel pairs
60 parameters	Flack parameter = 0.017 (15)
$w = 1/[\sigma^2(F_o^2) + (0.01P)^2$	
$+ 7.1387P]$	
where $P = (F_o^2 + 2F_c^2)/3$	

Compound (II) 293 K

Crystal data

$Rb_2Yb_{0.32}Ti_{1.68}(PO_4)_3$	$\lambda = 0.872$ Å
$M_r = 591.07$	Cell parameters from 4133
Cubic, $P2_13$	reflections
$a = 10.2132$ (2) Å	$\theta = 3.5$–34.1°
$V = 1065.33$ (4) Å^3	$\mu = 8.12$ mm^{-1}
$Z = 4$	$T = 293$ (2) K
$D_x = 3.664$ Mg m^{-3}	Plate, blue
Synchrotron radiation	$0.04 \times 0.04 \times 0.01$ mm

Data collection

Siemens SMART CCD	771 independent reflections
diffractometer	766 reflections with $F^2 > 2\sigma(F^2)$
ω scans	$R_{int} = 0.070$
Absorption correction: multi-scan	$\theta_{max} = 32.1°$
(*SADABS*; Sheldrick, 2001)	$h = -11 \rightarrow 12$
$T_{min} = 0.75$, $T_{max} = 0.96$	$k = -11 \rightarrow 11$
2811 measured reflections	$l = -12 \rightarrow 7$

Refinement

Refinement on F^2	$(\Delta/\sigma)_{max} < 0.001$
$R[F^2 > 2\sigma(F^2)] = 0.044$	$\Delta\rho_{max} = 0.98$ e Å^{-3}
$wR(F^2) = 0.118$	$\Delta\rho_{min} = -1.07$ e Å^{-3}
$S = 1.18$	Absolute structure: Flack (1983),
771 reflections	316 Friedel pairs
61 parameters	Flack parameter = 0.41 (3)
$w = 1/[\sigma^2(F_o^2) + (0.0654P)^2$	
$+ 5P]$	
where $P = (F_o^2 + 2F_c^2)/3$	

inorganic compounds

Compound (II) 150 K

Crystal data

$Rb_2Yb_{0.32}Ti_{1.68}(PO_4)_3$	$\lambda = 0.872$ Å
$M_r = 591.07$	Cell parameters from 7416
Cubic, $P2_13$	reflections
$a = 10.2228\,(5)$ Å	$\theta = 3.5–31.1°$
$V = 1068.34\,(9)$ Å^3	$\mu = 8.10$ mm^{-1}
$Z = 4$	$T = 150\,(2)$ K
$D_x = 3.675$ Mg m^{-3}	Plate, blue
Synchrotron radiation	$0.04 \times 0.04 \times 0.01$ mm

Data collection

Bruker SMART CCD	785 independent reflections
diffractometer	784 reflections with $F^2 > 2\sigma(F^2)$
ω scans	$R_{int} = 0.085$
Absorption correction: multi-scan	$\theta_{max} = 34.1°$
(*SADABS*; Sheldrick, 2001)	$h = -12 \rightarrow 13$
$T_{min} = 0.75$, $T_{max} = 0.96$	$k = -13 \rightarrow 12$
7663 measured reflections	$l = -12 \rightarrow 12$

Refinement

Refinement on F^2	$(\Delta/\sigma)_{max} < 0.001$
$R[F^2 > 2\sigma(F^2)] = 0.024$	$\Delta\rho_{max} = 0.62$ e Å^{-3}
$wR(F^2) = 0.063$	$\Delta\rho_{min} = -0.47$ e Å^{-3}
$S = 1.21$	Absolute structure: Flack (1983),
785 reflections	325 Friedel pairs
61 parameters	Flack parameter = 0.42 (2)
$w = 1/[\sigma^2(F_o^2) + (0.0264P)^2$	
$+ 1.609P]$	
where $P = (F_o^2 + 2F_c^2)/3$	

Table 1
Selected bond distances (Å) for (I) and (II) at 293 and 150 K.

	(I) 293 K	(I) 150 K	(II) 293 K	(II) 150 K
Yb1/Ti1—O1	2.115 (5)	2.113 (4)	2.107 (8)	2.115 (4)
Yb1/Ti1—O2	2.128 (5)	2.128 (5)	2.149 (8)	2.136 (5)
Yb2/Ti2—O3	2.019 (6)	2.017 (5)	2.054 (9)	2.035 (5)
Yb2/Ti2—O4^{viii}	2.041 (5)	2.039 (4)	2.046 (8)	2.039 (5)

Symmetry code as in Fig. 1.

Table 2
Bond-valence sums for (I) and (II).

	(I) 293 K	(I) 150 K	(II) 293 K	(II) 150 K
Rb1	1.06	1.06	1.04	1.06
Rb2	0.82	0.83	0.86	0.85
Yb1	3.93	3.94	3.87	3.95
Ti1^{IV}	2.62	2.63	2.58	2.60
Ti1^{III}	–	–	2.42	2.43
Yb2	5.00	5.06	4.78	4.93
Ti2^{IV}	3.36	3.38	3.18	3.31
Ti1^{III}	–	–	2.98	3.08
P	5.10	5.05	5.22	5.04

The data for (II) were collected at the Max II beamline 711 (Cerenius *et al.*, 2000). For (II), anomalous scattering factors for neutral atoms were taken from Sasaki (1989) and the linear absorption coefficients μ were calculated using mass attenuation coefficients from Sasaki (1990), both at wavelength 0.872 Å. The coordinates of (I) were used as starting points for the refinement of (II). The refinements of both (I) and (II) indicated mixed Yb/Ti populations of the two octahedral sites, as shown by the fact that the M—O bonds are longer than Ti^{iv}—O bonds (2.01 Å; Shannon, 1976). This difference was more pronounced for the M1 site. The existence of Yb/Ti mixing was also supported by the observation of excess-electron density at both sites when 100% Ti occupancies were used. The displacement parameters of the M sites were kept equal to ensure a stable refinement. The rubidium cation occupancies were initially set to refine freely but remained near full occupancy and were fixed at 1.00. For (II), ionic scattering factors for Ti^{4+}, Ti^{3+} and Yb^{3+} were tried but did not improve the model. The Flack (1983) parameter of (II) showed that the other absolute configuration was dominant, relative to (I), and the coordinates of (II) where therefore inverted and the asymmetric unit moved into the unit cell by translation. The twin refinement of (II) was performed using the *WinGX* program suite (Farrugia, 1999).

For compound (I) at 293 K, data collection: *SMART* (Siemens, 1995); cell refinement: *SAINT* (Siemens, 1995); data reduction: *SAINT* and *SADABS* (Sheldrick, 2001); program(s) used to solve structure: *SHELXS97* (Sheldrick, 1997). For compound (I) at 150 K, data collection: *SMART* (Siemens, 1995); cell refinement: *SAINT-Plus* (Bruker, 1999); data reduction: *SAINT-Plus* and *SADABS*; program(s) used to solve structure: coordinates from (I) at 293 K. For compound (II) at 293 K, data collection: *SMART-NT* (Bruker, 1998); cell refinement: *SAINT-Plus* (Bruker, 1999); data reduction: *SAINT-Plus*; program(s) used to solve structure: coordinates from (I). For compound (II) at 150 K, data collection: *SMART-NT*; cell refinement: *SAINT-Plus*; data reduction: *SAINT-Plus* and *SADABS*; program(s) used to solve structure: coordinates from (II) at 293 K. For both compounds at both temperatures, program(s) used to refine structure: *SHELXL97* (Sheldrick, 1997); molecular graphics: *ORTEP-3 for Windows* (Farrugia, 1997) and *DIAMOND* (Brandenburg, 2000); software used to prepare material for publication: *WinGX* (Farrugia, 1999).

References

Abrahams, S. C. & Bernstein, J. L. (1977). *J. Chem. Phys.* **67**, 2146–2150.
Alpen, U. von, Bell, M. F. & Wichelhaus, W. (1979). *Mater. Res. Bull.* **14**, 1317–1322.
Brandenburg, K. (2000). *DIAMOND.* Version 2.1d. Crystal Impact GbR, Bonn, Germany.
Brezina, B. & Glogarova, M. (1972). *Phys. Status Solidi A,* **11**, K39–K42.
Brown, I. D. (1981). *Struct. Bonding Cryst.* **2**, 1–30.
Brown, I. D. & Altermatt, D. (1985). *Acta Cryst.* B**41**, 244–247.
Bruker (1998). *SMART-NT.* Version 5.050. Bruker AXS Inc., Madison, Wisconsin, USA.
Bruker (1999). *SAINT-Plus.* Version 6.01 (includes *XPREP* and *SADABS*). Bruker AXS Inc., Madison, Wisconsin, USA.
Carvajal, J. J., Aznar, A., Sole, R., Gavalda, J., Massons, J., Solans, X., Auguillo, M. & Diaz, F. (2003). *Chem. Mater.* **15**, 204–211.
Cerenius, Y., Stahl, K., Svensson, L. A., Ursby, T., Oskarsson, A., Albertsson, J. & Liljas, A. (2000). *J. Synchrotron Rad.* **7**, 203–208.
Farrugia, L. J. (1997). *J. Appl. Cryst.* **30**, 565.
Farrugia, L. J. (1999). *J. Appl. Cryst.* **32**, 837–838.
Flack, H. D. (1983). *Acta Cryst.* A**39**, 876–881.
Guelylah, A., Madariaga, G., Morgenroth, W., Aroyo, M. I., Breczewski, T. & Bocanegra, E. H. (2000). *Acta Cryst.* B**56**, 921–935.

Jona, F. & Pepinsky, R. (1956). *Phys. Rev.* **103**, 1126–1130.

Leclaire, A., Benmoussa, A., Borel, M. M., Grandin, A. & Raveau, B. (1989). *J. Solid State Chem.* **78**, 227–231.

Lissalde, F., Abrahams, S. C., Bernstein, J. L. & Nassau, K. (1979). *J. Appl. Phys.* **50**, 845–851.

Lunezheva, E. S., Maksimov, B. A., Mel'nikov, O. K. & Muradyan, L. A. (1989). *Kristallografiya*, **34**, 611–614.

Masse, R., Durif, A., Guitel, J. C. & Tordjman, I. (1972). *Bull. Soc. Fr. Mineral Cristallogr.* **95**, 47–55.

Moriyoshi, C., Itoh, K. & Hikita, T. (1996). *Physica B*, **219/220**, 602–604.

Norberg, S. T. (2002). *Acta Cryst.* B**58**, 743–749.

O'Keeffe, M. & Andersson, S. (1977). *Acta Cryst.* A**33**, 914–923.

Percival, M. J. L., Schmahl, W. W. & Salje, E. (1989). *Phys. Chem. Miner.* **16**, 569–575.

Rao, G. H., Bämer, K. & Brown, I. D. (1998). *J. Phys. Condens. Matter*, **10**, 757–763.

Salinas-Sanchez, A., Garcia-Munoz, J. L., Rodriguez-Carvajal, J., Saez-Puche, R. & Martinez, J. L. (1992). *J. Solid State Chem.* **100**, 201–211.

Sasaki, S. (1989). KEK Report 88-14, pp. 1–136. National Laboratory for High Energy Physics, Tsukuba, Japan.

Sasaki, S. (1990). KEK Report 90-16, pp. 1–143. National Laboratory for High Energy Physics, Tsukuba, Japan.

Satyanarayan, M. N., Deepthy, A. N. & Bhat, H. L. (1999). *Crit. Rev. Solid State Mater. Sci.* **24**, 103–189.

Shannon, R. D. (1976). *Acta Cryst.* A**32**, 751–767.

Sheldrick, G. M. (1997). *SHELXL97* and *SHELXS97*. University of Göttingen, Germany.

Sheldrick, G. M. (2001). *SADABS*. Version 2.03. University of Göttingen, Germany.

Siemens (1995). *SMART* and *SAINT*. Siemens Analytical X-ray Instruments Inc., Madison, Wisconsin, USA.

Sljukic, M., Matkovic, B., Prodic, B. & Scavnicar, S. (1967). *Croat. Chem. Acta*, **39**, 145–148.

Slobodyanik, N. S., Stus, N. V., Nagornyi, P. G. & Kapshuk, A. A. (1991). *Russ. J. Inorg. Chem.* **36**, 1554–1556.

Thomas, P. A., Mayo, S. C. & Watts, B. E. (1992). *Acta Cryst.* B**48**, 401–407.

Zemann, A. & Zemann, J. (1957). *Acta Cryst.* **10**, 409–413.